



Visible photoluminescence from MgAl₂O₄ spinel with cation disorder and oxygen vacancy

Sawai, Shigeto
Uchino, Takashi

(Citation)

Journal of Applied Physics, 112(10):103523-103523

(Issue Date)

2012-11-15

(Resource Type)

journal article

(Version)

Version of Record

(Rights)

©2012 American Institute of Physics. This article may be downloaded for personal use only. Any other use requires prior permission of the author and the American Institute of Physics. The following article appeared in Journal of Applied Physics 112(10), 103523 and may be found at <http://dx.doi.org/10.1063/1.4767228>

(URL)

<https://hdl.handle.net/20.500.14094/90002687>



Visible photoluminescence from MgAl_2O_4 spinel with cation disorder and oxygen vacancy

Shigeto Sawai and Takashi Uchino

Citation: [Journal of Applied Physics](#) **112**, 103523 (2012); doi: 10.1063/1.4767228

View online: <http://dx.doi.org/10.1063/1.4767228>

View Table of Contents: <http://scitation.aip.org/content/aip/journal/jap/112/10?ver=pdfcov>

Published by the [AIP Publishing](#)

Articles you may be interested in

[Formation of the dopant-oxygen vacancy complexes and its influence on the photoluminescence emissions in Gd-doped \$\text{HfO}_2\$](#)

J. Appl. Phys. **116**, 123505 (2014); 10.1063/1.4896371

[Non-rare earth white emission phosphor: Ti-doped \$\text{MgAl}_2\text{O}_4\$](#)

Appl. Phys. Lett. **102**, 031104 (2013); 10.1063/1.4788929

[Ab initio many-body study of the electronic and optical properties of \$\text{MgAl}_2\text{O}_4\$ spinel](#)

J. Appl. Phys. **111**, 043516 (2012); 10.1063/1.3686727

[Magnetic and structural studies of the Verwey transition in \$\text{Fe}_{3-\delta}\text{O}_4\$ nanoparticles](#)

J. Appl. Phys. **95**, 7540 (2004); 10.1063/1.1669344

[On the cation distribution in \$\text{Ni}_{1-x}\text{Cu}_x\text{Fe}_{2-y}\text{Al}_y\text{O}_4\$ spinels](#)

J. Appl. Phys. **85**, 325 (1999); 10.1063/1.369450

A promotional banner for the Journal of Applied Physics. It features the AIP logo and the journal title at the top. Below this, the text 'Meet The New Deputy Editors' is centered. At the bottom, there are three circular headshots of the new deputy editors, each with their name written to the right: Christian Brosseau, Laurie McNeil, and Simon Phillpot. The background is a vibrant orange with a pattern of colorful, abstract spots.

Visible photoluminescence from MgAl_2O_4 spinel with cation disorder and oxygen vacancy

Shigeto Sawai and Takashi Uchino^{a)}*Department of Chemistry, Graduate School of Science, Kobe University, Nada, Kobe 657-8501, Japan*

(Received 30 August 2012; accepted 26 October 2012; published online 26 November 2012)

Magnesium aluminate spinel, MgAl_2O_4 , is a structurally and compositionally interesting crystal since it can exhibit significant deviations from the stoichiometric composition because of the ability of the lattice to tolerate substantial cation disorder. We show that MgAl_2O_4 spinels with excess Al_2O_3 non-stoichiometry can accommodate a large amount of positively charged oxygen vacancies (F^+ centers) when they are heated under vacuum at $\sim 1900^\circ\text{C}$ using a high-frequency induction heating unit with a graphite crucible. Thus the obtained spinels show a bluish white photoluminescence (PL) with a PL quantum yield of $\sim 20\%$, which is attributed to excitation and recombination processes of the F^+ center. The PL signal is characterized by a broad spectral band peaking at $\sim 2.7\text{ eV}$ ($\sim 460\text{ nm}$) and decays in a nonexponential manner on the time scale of several tens of microseconds. The F^+ center is supposed to interact with nearby positively and negatively charged defects derived from cation disorder in the spinel structure, forming clusters of various defect centers. © 2012 American Institute of Physics. [<http://dx.doi.org/10.1063/1.4767228>]

I. INTRODUCTION

Defects in metal oxide-based materials can strongly affect structural, optical, electronic, and dielectric properties of the host oxides.¹ Thus the amount of intrinsic and/or extrinsic defects should be decreased as low as possible to obtain high quality crystals. However, defects are not always harmful. For example, oxygen vacancies in simple oxides such as MgO and Al_2O_3 generally yield optical absorption bands in the 3–6 eV range, resulting in a variety of emission bands in the ultraviolet (UV)/visible region.^{2–4} Recently, oxygen vacancy-related emissions in MgO and Al_2O_3 have attracted renewed interest in view of dosimetric applications^{5,6} and broadband laser emission.^{7–9} In contrast to MgO and Al_2O_3 , magnesium aluminate spinel (MgAl_2O_4) generally exhibits quite a low luminescence efficiency ascribed to intrinsic oxygen vacancies.^{10,11} Such a low emission efficiency of oxygen vacancies in MgAl_2O_4 implies that only those oxygen vacancies in a particular configuration decay radiatively,¹⁰ although its mechanisms has not been well understood.

The characteristic structural feature peculiar to MgAl_2O_4 is its ability to tolerate cation disorder or to incorporate various cation species of different valence states into tetrahedral and octahedral positions, resulting in positively and negatively charged antisite defects.^{12–14} Consequently, MgAl_2O_4 provides exceptional structural stability against temperature, pressure, and high-energy radiation.¹⁵ Thus, if the low emission efficiency of oxygen vacancies in MgAl_2O_4 can be somehow improved, this will open up promising prospects for physically robust light-emitting materials containing no metal activator ions.

In this work, we demonstrate that the emission quantum efficiency of MgAl_2O_4 can be raised to $\sim 20\%$ when the

positively charged oxygen vacancy (the F^+ center, the oxygen vacancy with one electron) rather than the neutrally charged oxygen vacancy (the F center, the oxygen vacancy with two electrons) is introduced into the spinel structure. The introduction of the F^+ and F centers was accomplished by heating MgAl_2O_4 powders under vacuum conditions with a high-frequency induction heating unit, which allows us to control stoichiometry and cation disorder in the spinel structure. A possible structural environment of the F^+ center responsible for the emission in the visible spectral region is also discussed.

II. EXPERIMENTAL PROCEDURES

Starting magnesium aluminate spinel powders were prepared by heating mixtures of MgO (99.99%) and Al_2O_3 (99.99%) powders, with different $\text{Al}_2\text{O}_3/\text{MgO}$ ratios (x_1) ranging from 0.67 to 1.8. The oxide mixtures were sintered for a period of 5 h at 1700°C in air using an electric furnace. Since these as-prepared spinel samples hardly contain intrinsic oxygen vacancies or luminescent centers, we then heated these as-sintered powders under highly reducing conditions using a graphite crucible and a high-frequency induction heating unit, which is rated at 4 kW at a maximum frequency of 420 kHz, under continuous evacuation with a turbo molecular pump down to $\sim 10^{-3}\text{ Pa}$. The graphite crucible is used not only as an electrically conductive object for induction heating but also as a reducing agent. Recently, we have reported that this vacuum heating process with a graphite crucible is useful to introduce a large amount ($\sim 10^{17}\text{ cm}^{-3}$) of oxygen vacancies in high-melting temperature oxides such as $\alpha\text{-Al}_2\text{O}_3$.¹⁶ The heating temperature was raised up to $\sim 1900^\circ\text{C}$ at a rate of $\sim 500^\circ\text{C}/\text{min}$ and maintained at the same temperature for 3 min. The temperature of the system was monitored with a radiation thermometer. During the induction heating, the sample powders ($\sim 1.0\text{ g}$) were melted,

^{a)}Author to whom correspondence should be addressed. Electronic mail: uchino@kobe-u.ac.jp.

accompanied by the partial vaporization of constituent oxides, which is manifested as a total weight loss of ~ 10 wt. %. After the induction heating process, the sample was allowed to cool to room temperature, forming a translucent sphere-shaped solid with diameter of ~ 10 mm [see Figure 1(a)]. Thus the obtained solid samples were crushed into powders for XRD and photoluminescence (PL) measurements.

X-ray diffraction patterns of the crushed samples were obtained using a powder x-ray diffractometer (Rigaku, SmartLab) using $\text{Cu K}\alpha$ (1.541 \AA) radiation. Diffraction signals were measured for a 2θ range $3\text{--}158^\circ$ at an angular resolution of 0.02° . For the measurements of steady state PL spectra, we used a spectrofluorometer (JASCO, FP 6600) using a xenon lamp for excitation. A series of PL data for different samples were acquired under the same detection condition and optical setup. Scans were performed at 200 nm/min with the excitation and emission band passes set at 3 and 6 nm , respectively. Temperature dependence of the steady state PL spectra was obtained by using a closed-cycle N_2 cryostat in the temperature range from 77 to 450 K . The absolute PL quantum yield ϕ was also obtained based on the measurement with an integrated sphere system,¹⁷ which was calibrated with a standard light source; ϕ was defined as the number of photons emitted in PL per absorbed photon. The experimental error of the quantum yield obtained in the present system was within $\pm 0.5\%$.

For time-resolved PL measurements, we used a gated image-intensified charge-coupled device (Princeton Instruments, PI-MAX:1024RB) and a 150 lines/mm grating by using the fourth harmonic (266 nm) of a pulsed Nd: yttrium aluminum garnet (YAG) laser (Spectra Physics, INDI 40, pulse width 8 ns , repetition rate 10 Hz).

III. RESULTS

Figure 2 shows the XRD patterns of the induction heated samples with different initial $\text{Al}_2\text{O}_3/\text{MgO}$ batch ratios (x_1). All the observed peaks were indexed to the XRD pattern of magnesium aluminate spinel. The values of the refined lattice constant a_0 are also given in Fig. 2. We found that the peak positions (lattice constant) tend to shift to higher angles (smaller values) with increasing the x_1 value. The $\text{Al}_2\text{O}_3/\text{MgO}$ ratio of the thus obtained samples can be more reasonably estimated from the observed lattice constant using the following empirical equation:^{18,19}

$$x_2 = (8.6109 - a_0)/(3a_0 - 23.7195), \quad (1)$$

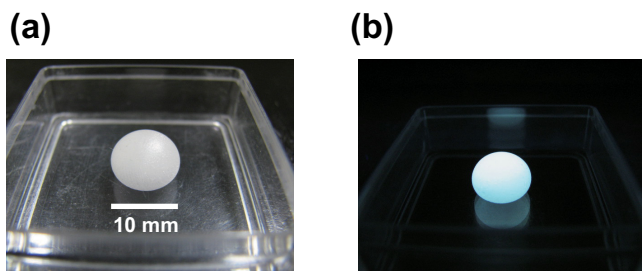


FIG. 1. Photographs of an induction heated sample ($x_2 = 2.39$) under (a) normal light and (b) ultraviolet (UV) illumination with a 254 nm hand-held UV lamp in the dark.

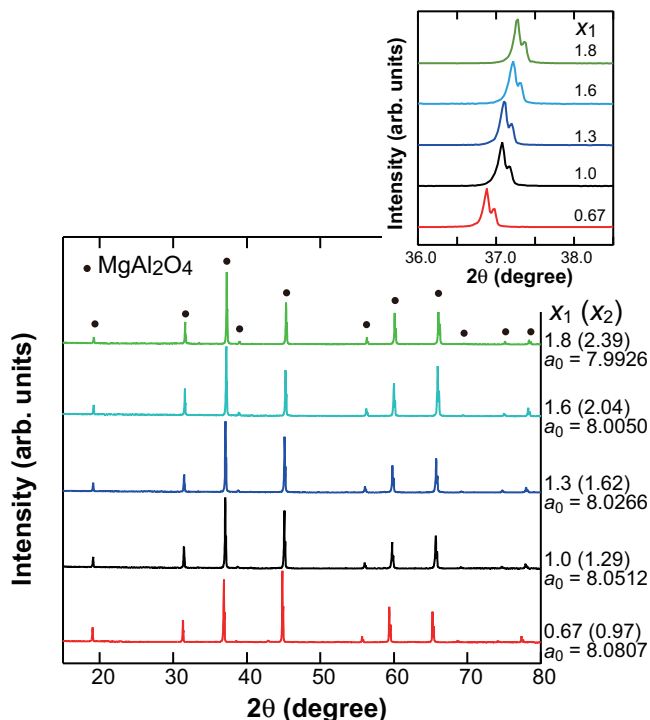


FIG. 2. XRD patterns of the induction heated samples with different initial $\text{Al}_2\text{O}_3/\text{MgO}$ batch ratios (x_1). The inset shows an expanded plot for $2\theta = 36.0\text{--}38.5^\circ$. The refined lattice constant a_0 and the $\text{Al}_2\text{O}_3/\text{MgO}$ ratio estimated from Eq. (1) (x_2) are also shown.

where a_0 is the lattice constant in \AA . As shown in Fig. 2, the x_2 value estimated from Eq. (1) is larger than that of the starting batch composition (x_1) by $\sim 0.2\text{--}0.5$. This implies the preferential evaporation of MgO under high reducing atmosphere, in agreement with previous observations.^{19–21} In what follows, we use the x_2 value to designate the type of induction heated samples.

We next turn to the photoluminescence characteristics. Initial air-sintered spinel powders hardly show photoluminescence signals under UV excitation, as indeed expected from previous observations.^{10,11} However, the induction heated samples tend to exhibit a bluish-white emission under UV excitation of $4\text{--}6 \text{ eV}$ [see Figure 1(b)]. The highest PL quantum yield ($19.4 \pm 0.5\%$) was obtained for the sample $x_2 = 2.39$. Figure 3 shows PL excitation (PLE) spectra for several induction heated samples. The PLE spectra are characterized by a highly asymmetrical shape, which can be deconvoluted into two Gaussian components centered at ~ 4.8 and $\sim 5.3 \text{ eV}$. Although the relative weight of the two components varies depending on the x_2 value, the variations of the peak position for the $\sim 4.8\text{-}$ and $\sim 5.3\text{-eV}$ bands are less than 0.15 and 0.08 eV , respectively. These PLE components are well compared with the optical absorption bands of the F^+ (4.75 eV) and F (5.3 eV) centers reported previously for MgAl_2O_4 .^{22,23} We hence attributed the observed $\sim 4.8\text{-}$ and $\sim 5.3\text{-eV}$ PLE components to the F^+ and F centers, respectively.

Figure 4(a) shows the PL spectra of the sample with $x_2 = 2.39$ under excitation with lights of 4.66 and 5.23 eV , which are the peak energies of the corresponding PLE spectrum shown in Fig. 3(c). In Fig. 4(a), each spectrum is normalized to unity at the peak energy. One sees from Fig. 4(a) that the

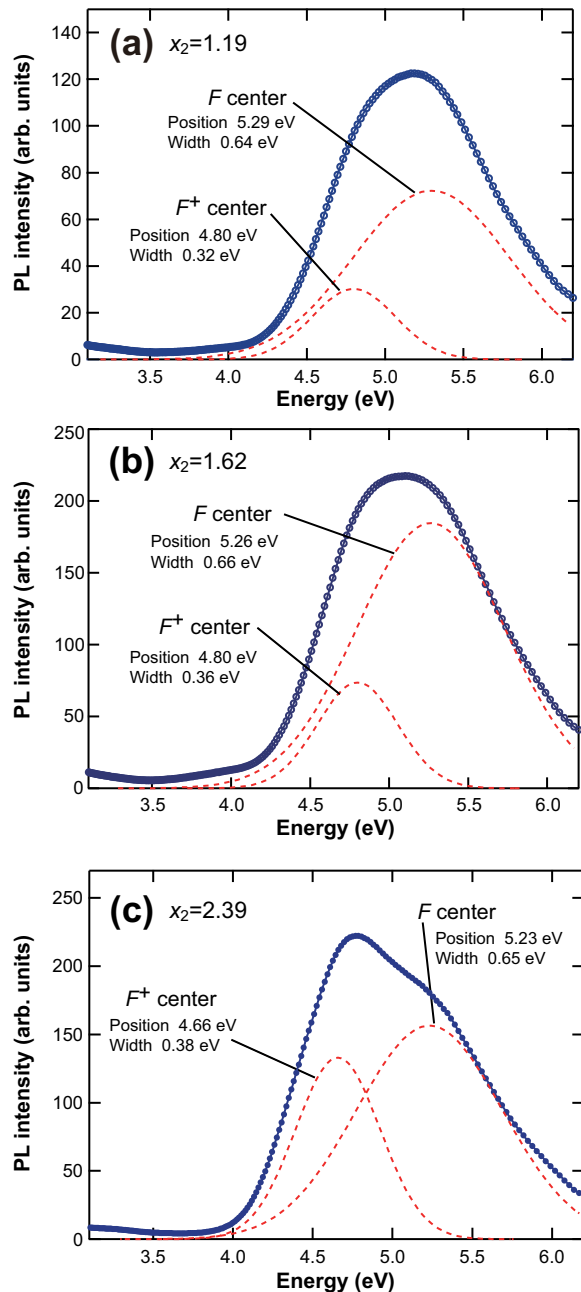


FIG. 3. Photoluminescence excitation spectra for the 2.7-eV PL band of the induction heated samples with (a) $x_2 = 1.19$, (b) $x_2 = 1.62$, and (c) $x_2 = 2.39$. The red dotted lines represent the results of Gaussian curve fitting.

observed PL spectra are basically identical to each other irrespective of the excitation energy, showing the common PL peak energy at ~ 2.7 eV. This strongly suggests that the photoexcitation of the F and F^+ centers eventually results in the same radiative relaxation channel. As shown in the inset of Fig. 4(a), the PL intensity is substantially reduced when the induction heated sample is post-annealed in air at 1500°C for 15 h. This allows us to assume that oxygen vacancies are responsible for the ~ 2.7 eV PL band.

Figure 4(b) shows the PL spectra of the samples with different values of x_2 . The peak position of the ~ 2.7 eV PL band shows an almost linear variation with the x_2 value [see also the inset of Fig. 4(b)], implying that the emission energy level is affected by the $\text{Al}_2\text{O}_3/\text{MgO}$ ratio in the spinel sample.

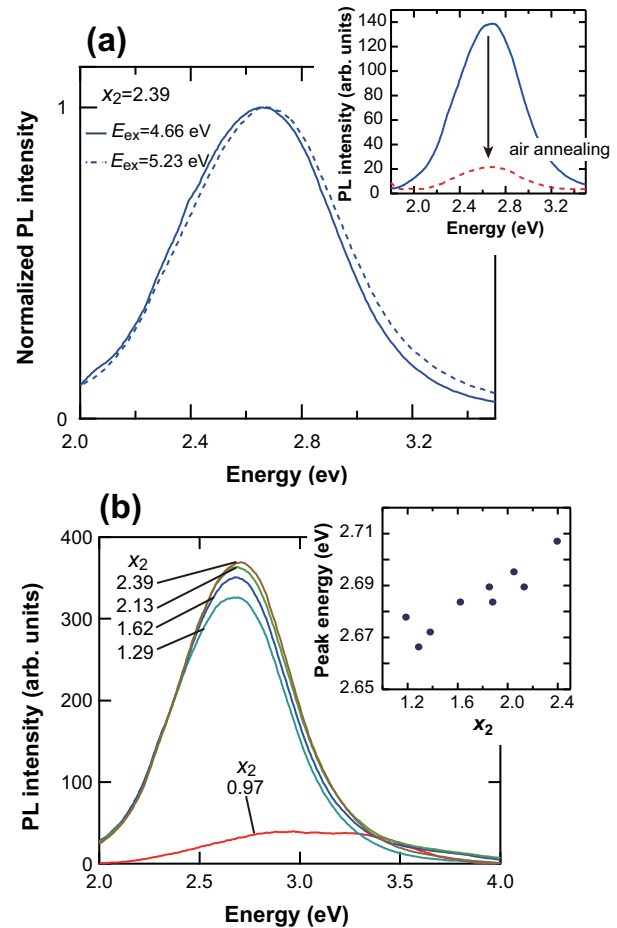


FIG. 4. (a) Normalized PL spectra of the induction heated sample with $x_2 = 2.39$ under excitation of light of different energies. The inset of panel (a) shows the PL spectra before (blue solid line) and after (red dotted line) annealing in air at 1500°C for 15 h. (b) PL spectra of the induction heated samples with different values of x_2 . The excitation energy was 4.7 eV. The inset of panel (b) shows changes in the peak position with x_2 for the samples with $x_2 > 1$.

It should be noted, however, that the PL intensity of the sample with $x_2 = 0.97$ is rather low, showing no well-defined PL peaks. It is hence probable that a certain oxygen vacancy site in alumina-rich spinel samples ($x_2 > 1$) is responsible for the visible PL emission at ~ 2.7 eV.

A typical PL decay profile measured for the ~ 2.7 eV PL band is given in Figure 5. The PL signal decays non-exponentially on the time scale of several tens of microseconds. We found that the decay profile is well fitted to a triple exponential function with time constants of 3.5, 9.3, and 46.3 μs . Such a highly nonexponential decay behavior implies that the relevant emission process experiences multiple trapping and detrapping events before the radiative recombination process occurs.^{24,25} The expected multiple relaxation events can also be deduced from the temperature dependence of the PL intensity I (see Figure 6), which can be represented by the following equation assuming two nonradiative recombination channels,²⁶

$$I(T) = \frac{I_0}{1 + A_1 \exp(-E_1/kT) + A_2 \exp(-E_2/kT)}, \quad (2)$$

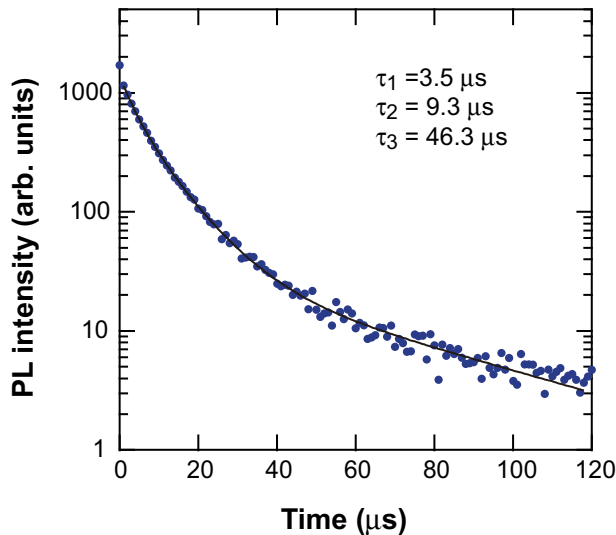


FIG. 5. PL decay profile at 2.7 eV for the induction heated sample with $x_2 = 2.39$ measured at room temperature. The fourth harmonic of the pulsed Nd:YAG laser ($\lambda = 266$ nm, 4.66 eV) is used as an excitation source. The solid line indicates the result of least-square fitting to a triple-exponential function, and the fitted decay time constants are also shown.

where E_1 and E_2 are the activation energies of the two competitive nonradiative recombination processes, I_0 is the intensity at zero temperature, k is the Boltzmann constant, and A_1 and A_2 are fitting constants. The curve fitting gives rise to two typical activation energies of ~ 400 and ~ 50 meV. The existence of the second nonradiative activation channel suggests that, in addition to the emission center, there exists an alternative nonradiative recombination center that contributes to the entire relaxation process. It is reasonable to assume that the additional nonradiative recombination center can also behave as a trapping center, which can be responsible for the highly nonexponential decay behavior (Figure 5).

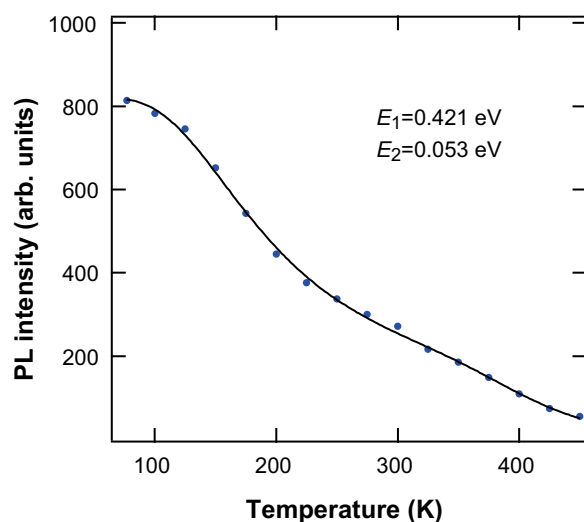


FIG. 6. Temperature dependence of the PL intensity at 2.7 eV for the induction heated sample with $x_2 = 2.39$. The solid line indicates the result of least-square fitting to Eq. (2). Fitted values of the activation energies (E_1 and E_2) for the two nonradiative recombination processes are also shown.

IV. DISCUSSION

Thus, the present observations have revealed the following points concerning the ~ 2.7 -eV PL band of the induction heated MgAl_2O_4 spinels.

- (1) The PL spectral shape depends hardly on the excitation energy [Figure 4(a)].
- (2) The PL signal is observed only from the samples with $x_2 > \sim 1$, and the PL peak energy increases with increasing the x_2 value [Figure 4(b)].
- (3) The radiation recombination process is accompanied by multiple trapping and multiple nonradiative recombination processes (Figures 5 and 6).

From these results, we will discuss a possible structural origin of the ~ 2.7 eV PL band. The peak energy of the present PL band is quite similar to that (2.69 eV) observed previously from thermochemically reduced MgAl_2O_4 single crystals.¹⁰ As mentioned previously, however, the emission quantum yield of the thermochemically reduced MgAl_2O_4 is reported to be quite low (less than one-tenth that of the F -center luminescence in MgO ¹⁰), in contrast to our samples with rather a high PL quantum yield of $\sim 20\%$. What is the difference between our samples and the previous thermochemically reduced ones? It is interesting to point out that the PLE spectra of our samples are quite different from that of the thermochemically reduced MgAl_2O_4 sample. As shown in Fig. 3, our samples exhibit two comparable PLE components centered at ~ 4.8 and ~ 5.3 eV, which are ascribed to the F^+ and F centers, respectively. On the other hand, the PLE spectrum of the thermochemically reduced sample has a dominant peak at ~ 5.3 eV attributed to the F center; there is a small secondary maximum at ~ 4.45 eV, but this is only $\sim 7\%$ of the main peak.¹⁰ These results strongly suggest that the color center that is responsible for the ~ 2.7 -eV PL band is not the F center but the F^+ center, as will be discussed further below.

As mentioned above, the F center is the principal oxygen vacancy center in thermochemically reduced oxides such as MgO , $\alpha\text{-Al}_2\text{O}_3$, and MgAl_2O_4 .^{2,3,10,27} That is, the concentration of the positively charged F^+ center is quite low, or sometimes zero, in thermochemically reduced oxides. It has been demonstrated that the excited state of the F center in these oxides is located just below the bottom of the conduction band.^{2,10,22} This allows the electron in the excited state to escape easily into the conduction band, resulting in the following photoionization process^{2,10,22}

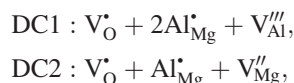


The resulting electrons can be, in principle, monitored by photoconductivity measurements. Indeed, the excitation wavelength dependence of the photocurrent of thermochemically reduced MgAl_2O_4 exhibit two peaks at 5.39 and 4.59 eV, which are attributed to the photoionization processes of the F center and an unidentified electron trap such as Fe, respectively.¹⁰ It has been found, however, that the photocurrent peak at 5.39 eV is easily bleached because of the presence of certain electron trapping sites.¹⁰ Although

similar bleaching effects are observed in the photocurrent spectra of the F centers in other oxides, the bleaching behavior is particularly pronounced in MgAl_2O_4 .¹⁰ This suggests that positively charged antisite defects in the spinel structure, i.e., Al^{3+} in tetrahedral Mg^{2+} sites, are responsible for the electron trapping and the related bleaching processes. If the above photoionization and electron trapping processes dominate over the radiative recombination process during the photoexcitation of the F center, the F center cannot behave as an emission center, probably explaining the reason for a low efficiency for an F -center luminescence in MgAl_2O_4 .^{10,11} On the other hand, the excited state of the F^+ center in oxides is generally located well below the bottom of the conduction band, and the photoionization and the related photobleaching of the F^+ center will rarely occur.^{2,28} Thus, a high PL quantum yield will be anticipated for the spinels containing a large amount of F^+ centers. The observed excitation energy independence of the ~ 2.7 -eV PL band (point 1 mentioned earlier) is also consistent with our assumption that the F^+ center is the only emission center in MgAl_2O_4 . We should note, however, that the excited state of the F^+ center will be realized not only by the direct photoexcitation of the F^+ center but also, although temporally, by the photoionization of the F center, yielding the two PLE components at ~ 4.8 and ~ 5.3 eV, as shown in Fig. 3.

The F^+ -center emission model can further account for the composition dependence of the PL intensity and peak energy shown in Fig. 4(b) (point 2). The introduction of the F^+ center must be accompanied by simultaneous introduction of some negatively charged centers. It is also interesting to point out that for the spinel samples with $x_2 > 1$, excess Al^{3+} ions will replace Mg^{2+} ions, and charge neutrality will be maintained by the formation of negatively charged centers such as Al and Mg vacancies.^{29–31} In other words, negatively charged centers are inherently present in the spinels with $x_2 > 1$. This allows us to assume that the samples with $x_2 > 1$ can accommodate a larger number of F^+ centers than those with $x_2 < 1$.

Thus, the F^+ center in MgAl_2O_4 should not be viewed as an isolated defect center but as defect clusters (DCs) consisting of various types of positively and negatively charged defects. The idea of DCs has been often used to evaluate the stability of antisite defects and their charge compensating point defects in spinels.^{30,32} Examples of the relevant DCs can be described as follows using the Kröger-Vink notation,



where $\text{V}_{\text{O}}^{\bullet}$, $\text{Al}_{\text{Mg}}^{\bullet}$, $\text{V}_{\text{Al}}^{\prime\prime\prime}$, and $\text{V}_{\text{Mg}}^{\prime\prime}$ indicate a singly positively charged oxygen vacancy or an F^+ center, a singly positively charged Al at a tetrahedral Mg site, a triply negatively charged Al vacancy, and a doubly negatively charged Mg vacancy, respectively. On the basis of the DC model, it would be reasonable to expect that the electronic state of $\text{V}_{\text{O}}^{\bullet}$ (F^+) is affected by the type and amount of nearby charged centers, resulting in the observed composition dependence of the F^+ -center related PL characteristics (point 2). Furthermore,

the electronic excitation of the F^+ center will not be confined to this single defect site but may be distributed over several defect sites. A photoexcited electron and a hole at the F^+ center will hence be trapped by a nearby positively charged site ($\text{Al}_{\text{Mg}}^{\bullet}$) and a negatively charged site ($\text{V}_{\text{Al}}^{\prime\prime\prime}$ or $\text{V}_{\text{Mg}}^{\prime\prime}$), respectively, via tunneling or hopping processes. These trapping sites could possibly become nonradiative recombination sites. Thus, the relaxation process of the F^+ center in DCs is presumably rather complex because of the surrounding charged defects, leading to multiple trapping and multiple nonradiative recombination processes (point 3).

V. CONCLUSION

We have shown that the induction heating with a graphite crucible under vacuum is a simple but efficient method to obtain luminescent MgAl_2O_4 spinel. It is most likely that the color center responsible for the ~ 2.7 -eV PL band is the positively charged F^+ center. On the other hand, the neutrally charged F center will hardly decay radiatively because of ionization of the F center during the photoexcitation process. Considering that the ~ 2.7 -eV PL band is observed by photoexcitation of both the F and F^+ centers, we suggest that the F^+ center induced by photoionization of the F center is partly responsible for the observed visible emission; however, the principal emission process will be the direct photoexcitation of the F^+ center. In the present induction heating process, a substantial amount of the F^+ center can be introduced into the alumina-rich spinels since excess Al^{3+} ions inherently provide negatively charged cation vacancies, $\text{V}_{\text{Al}}^{\prime\prime\prime}$ and $\text{V}_{\text{Mg}}^{\prime\prime}$, which are also expected to behave as charge compensators for the F^+ centers. In the spinel lattice, such charged defects as $\text{V}_{\text{O}}^{\bullet}$ (F^+ center), $\text{Al}_{\text{Mg}}^{\bullet}$, $\text{V}_{\text{Al}}^{\prime\prime\prime}$, and $\text{V}_{\text{Mg}}^{\prime\prime}$ will come close to each other, forming defect clusters. It can hence be understood that the oxygen-vacancy-related PL characteristics of MgAl_2O_4 are influenced not only by the type and amount of oxygen vacancies but also by those of antisite defects and cation vacancies or the degree of cation disorder in the spinel structure.

¹Y. M. Chiang, D. P. Birnie, and W. D. Kingery, *Physical Ceramics: Principles for Ceramic Science and Engineering* (Wiley, New York, NY, 1996).

²B. D. Evans, G. J. Pogatschnik, and Y. Chen, *Nucl. Instrum. Methods Phys. Res. B* **91**, 258 (1994).

³G. P. Summers, T. M. Wilson, B. T. Jeffries, H. T. Tohver, Y. Chen, and M. M. Abraham, *Phys. Rev. B* **27**, 1283 (1983).

⁴M. A. Monge, A. I. Popov, C. Ballesteros, R. González, Y. Chen, and E. A. Kotomin, *Phys. Rev. B* **62**, 9299 (2000).

⁵S. W. S. McKeever, *Nucl. Instrum. Methods Phys. Res. B* **184**, 29 (2001).

⁶E. G. Yuhikara and S. W. S. McKeever, *J. Appl. Phys.* **100**, 083512 (2006).

⁷T. Uchino and D. Okutsu, *Phys. Rev. Lett.* **101**, 117401 (2008).

⁸T. Uchino, D. Okutsu, R. Katayama, and S. Sawai, *Phys. Rev. B* **79**, 165107 (2009).

⁹Y. Uenaka and T. Uchino, *Phys. Rev. B* **83**, 195108 (2011).

¹⁰P. K. Bandyopadhyay and G. P. Summers, *Phys. Rev. B* **31**, 2422 (1985).

¹¹L. S. Cain, G. J. Pogatschnik, and Y. Chen, *Phys. Rev. B* **37**, 2645 (1988).

¹²K. E. Sickafus, J. M. Wills, and N. W. Grimes, *J. Am. Ceram. Soc.* **82**, 3279 (1999).

¹³S. A. T. Redfern, R. J. Harrison, H. St.C. O'Neill, and D. R. R. Wood, *Am. Mineral.* **84**, 299 (1999).

¹⁴B. P. Uberuaga, D. Bacorisen, R. Smith, J. A. Ball, and R. W. Grimes, *Phys. Rev. B* **75**, 104116 (2007).

- ¹⁵F. W. Clinard, G. F. Hurley, and L. W. Hobbs, *J. Nucl. Mater.* **108/109**, 655 (1982).
- ¹⁶M. Itou, A. Fujiwara, and T. Uchino, *J. Phys. Chem. C* **113**, 20949 (2009).
- ¹⁷N. C. Greenham, I. D. W. Samuel, G. R. Hayes, R. T. Phillips, Y. A. R. Kessener, S. C. Moratti, A. B. Holmes, and R. H. Friend, *Chem. Phys. Lett.* **241**, 89 (1995).
- ¹⁸H. U. Viertel and F. Seifert, *Neues Jahrb. Mineral., Abh.* **134**, 167 (1979).
- ¹⁹C.-J. Ting and H.-Y. Lu, *J. Am. Ceram. Soc.* **83**, 1592 (2000).
- ²⁰A. D. Mazzoni, M. A. Sainz, A. Caballero, and E. F. Aglietti, *Mater. Chem. Phys.* **78**, 30 (2003).
- ²¹T. Sasamoto, H. Hara, and T. Sata, *Bull. Chem. Soc. Jpn.* **54**, 3327 (1981).
- ²²G. P. Summers, G. S. White, K. H. Lee, and J. H. Crawford, Jr., *Phys. Rev. B* **21**, 2578 (1980).
- ²³A. Ibarra, D. Bravo, F. J. Lopez, and F. A. Garner, *J. Nucl. Mater.* **336**, 156 (2005).
- ²⁴M. S. Minsky, S. Watanabe, and N. Yamada, *J. Appl. Phys.* **91**, 5176 (2002).
- ²⁵T. Onuma, S. F. Chichibu, A. Uedono, T. Sota, P. Cantu, T. Katona, J. F. Keady, S. Keller, U. K. Mishra, S. Nakamura, and S. P. DenBaars, *J. Appl. Phys.* **95**, 2495 (2004).
- ²⁶M. Leroux, N. Grandjean, B. Beaumont, G. Nataf, F. Semond, J. Massies, and O. Gibart, *J. Appl. Phys.* **86**, 3721 (1999).
- ²⁷G. S. White, K. H. Lee, and J. H. Crawford, Jr., *Appl. Phys. Lett.* **35**, 1 (1979).
- ²⁸K. H. Lee and J. H. Crawford, Jr., *Phys. Rev. B* **19**, 3217 (1979).
- ²⁹R. I. Sheldon, T. Hartmann, K. E. Sickafus, A. Ibarra, B. L. Scott, D. N. Argyriou, A. C. Larson, and R. B. von Dreele, *J. Am. Ceram. Soc.* **82**, 3293 (1999).
- ³⁰S. T. Murphy, C. A. Gilbert, R. Smith, T. E. Mitchell, and R. W. Grimes, *Philos. Mag.* **90**, 1297 (2010).
- ³¹T. Soeda, S. Matsumura, C. Kinoshita, and N. J. Zaluzec, *J. Nucl. Mater.* **283–287**, 952 (2000).
- ³²C. A. Gilbert, R. Smith, S. D. Kenny, S. T. Murphy, R. W. Grimes, and J. A. Ball, *J. Phys.: Condens. Matter* **21**, 275406 (2009).